# Optimization Project Report

Aniket Bagade, Mit Phanase, Nachiket Soni, Naitik Dalwadi

March 21, 2025

**Abstract**

This work analyses the impact of different optimization algorithms on the performance and efficiency of compressors. The dataset used consists of points in the characteristic performance map. A custom evaluation metric is developed that helps to compare different configurations of 4 Optimizers and 3 error metrics. The optimization algorithms are implemented in Python and compared with respect to their error performance and number of iterations required to reach the solution. Moreover, the effect of different boundary conditions on the objective function are studied.

## 1 Introduction

Turbochargers play a crucial role in both automotive and marine diesel engines (Song et al., 2019). The physical data point collection for a compressor is an expensive endeavor and thus, conducting extensive experiments is not feasible. This neccessitates the development of a mathematical model with optimal predictive accuracy for their working cycle dynamics. The major mathematical modeling techniques of marine compressors lie under curve-fitting techniques, as they effectively capture the fundamental physical characteristics within the mathematical framework.

This study aims to identify a few suitable classical optimization algorithm for compressor datasets in terms of performance and efficiency. Furthermore, it examines the appropriate error metric for optimization and explores the determination of boundary conditions to achieve optimal results for compressor datasets.

The remainder of this paper is structured as follows: Section 2 provides an overview of various optimization algorithms and error metrics utilized in this study. Additionally, it discusses the boundary conditions for the $\beta$ parameters that require optimization. The evaluation metrics used to assess different configurations are also detailed in this section. Section 3 presents a comparative analysis of the results obtained from different configurations.

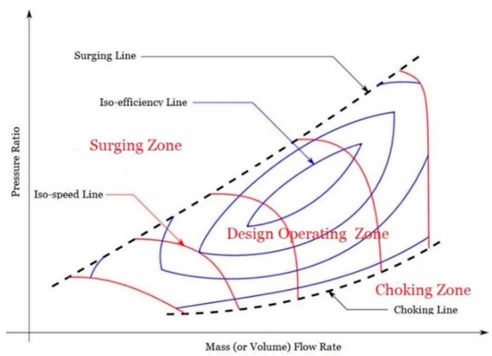


Figure 1: Compressor Performance Map

# 2 Methods

## 2.1 Compressor Characteristic Map: Speed-Line Modeling

The performance map of a compressor usually represents its working characteristic, as shown in figure 1. The horizontal and vertical axes represent the mass (or volume) flow rate and pressure ratio, respectively. The measured data points at the same rotational speed are connected in performance map, which forms iso-speed lines. Similarly, those data points with the same isentropic efficiency are connected, which forms iso-efficiency lines (Fang et al., 2014).

The compressor performance map is divided into following three zones:

- **Design Operating Zone**: It is the zone, where compressor works stably and achieve high efficiency.
- **Surging Zone**: In this zone, the compressor does not have sufficient amount of air at high pressure ratio, which leads to reverse flow of air and premature failure of the compressor. On each iso-speed line, the curve passes through the surge point is known as **surging line.**
- **Choking Zone**: In this zone, though the decrease in pressure ratio, the mass flow rate will not increase further and it flows at sonic velocity. On each iso-speed line, the curve passes through the choking point is known as **choking line.**

Based on the selection of the input and output parameters, the models are classified into two following categories:

$$\dot{m} = f(\Pi, N) \tag{1}$$

$$\Pi = f(\dot{m}, N) \tag{2}$$

Where, N is the rotational speed of the compressor, $\dot{m}$ is the mass flow rate, and $\Pi$ is the pressure ratio.

| Dataset | Summary Statistics | Pi_tot_V | m_V |
|---|---|---|---|
| experiment_0.1 | mean | 3.811611 | 5.198377 |
| | std | 1.278679 | 1.892726 |
| experiment_0.01 | mean | 3.805166 | 5.194258 |
| | std | 1.266266 | 1.895922 |
| experiment_0.001 | mean | 3.804175 | 5.194126 |
| | std | 1.266433 | 1.894269 |

Table 1: Summary Statistics of the Datasets

Moreover, Llamas Ellipse Model (Shen et al., 2019) is capable of working in both direction, which means it can predict either mass flow rate or pressure ratio based on the situation. In the design operating zone, the iso-speed line is represented by the super ellipse represents the relationship between $\dot{m}$ and $\Pi$

$$(\frac{\dot{m} - \dot{m_{zs}}}{\dot{m_{ch}} - \dot{m_{zs}}})^{CUR} + (\frac{\Pi - \Pi_{ch}}{\Pi_{zs} - \Pi_{ch}})^{CUR} = 1 \tag{3}$$

Where,

- $\dot{m_{zs}}$ is the mass flow rate at the surge point.
- $\dot{m_{ch}}$ is the mass flow rate at the choking point.
- $\Pi_{zs}$ is the pressure ratio at the surge point.
- $\Pi_{ch}$ is the pressure ratio at the choking point.
- $CUR$ is the curvature of the super ellipse.

These five parameters are encapsulated in ß parameter vector, and this parameter vector is optimized to minimize the error between the predicted and actual values of the mass flow rate and pressure ratio.

## 2.2 Data Sets

The three different datasets were used in this study. Each dataset consists of three columns: ***Speedclass[m/s]***, ***Pi_tot_V[-]***, and ***m_V[kg/s]***, and 63 rows contain empirical data of pressure ratio and mass flow rate at 10 different compressor speeds ranging from 3750 to 8550 m/s. Moreover, each dataset does not contain any missing values. The summary statics of the datasets are shown in Table 1.

As it is observed in the Table 1, the experiment_0.1 dataset has more dispersion, followed by the experiment_0.01 and experiment_0.001 datasets.

## 2.3 Optimization Algorithms

To analyze the effect of different optimization algorithms on the available compressor datasets, following four algorithms have been used from the Scipy Library (Virtanen et al., 2020):

- Nelder-Mead (Nelder and Mead, 1965)
- Powell (Powell, 1964)
- TNC (Nash, 1984)
- L-BFGS-B (Zhu et al., 1997)

Above listed all four optimization algorithms are local and deterministic. Moreover, Nelder-Mead and Powell algorithms do not need gradient of the objective function whereas TNC and L-BFGS-B algorithms require gradient of the objective function.

In this study, Nelder-Mead algorithm is used as reference algorithm, and the performance of the other three algorithms is compared with it. This study is focused on the following research question:

- Which optimization algorithm is most suitable for the available compressor data sets in terms of performance and efficiency?

## 2.4 Metrics

To analyze the impact of different metrics on the performance of the optimization algorithms, we used the following metrics:

- Orthogonal error (ortho): Calculates orthogonal difference between two points according to following equation:

$$ortho = \sum_{i=1}^{n} \left[ (\Delta x_i)^2 + (\Delta y_i)^2 \right] \tag{4}$$

  where $\Delta x_i$ is the difference in x coordinates of 2 points and $\Delta y_i$ is the difference in y coordinates of 2 points.

- $R^2$ score: Calculates coefficient of determination using following equation:

$$R^2 = 1 - \frac{\sum_{i=1}^{n} (y_i - \hat{y}_i)^2}{\sum_{i=1}^{n} (y_i - \bar{y})^2} \tag{5}$$

  where $n$ is the number of points in a speed line and $\bar{y}$ is the mean of the actual values.

- Mean Absolute Error (MAE): Calculates mean of absolute errors using equation given below:

$$MAE = \frac{1}{n} \sum_{i=1}^{n} |y_i - \hat{y}_i| \tag{6}$$

  where n is the number of points in a speed line.

### 2.5 Boundary Conditions

In this study, the default bounds are selected as the minimum and maximum values of Pi_tot_V and m_V, which are then scaled between 0.75 and 1.25. For CUR, the bounds are set between 2 and 15. Subsequently, the lower and upper bound are expanded by increasing their scaling factors by 0.25, and for CUR, we increase only the upper bound by 5. The mean of results are compared to determine optimal boundary conditions.

### 2.6 Evaluation

To compare the results of the different configurations (optimization algorithms, metrics, and boundary conditions), the following evaluation methods have been used:

- Number of Iterations: Number of iterations taken by the optimizer to reach the minimum of objective function per speedline.
- Overall RMSE: Overall normalised Root Mean Squared Error of the predicted values of mass flow rate and pressure ratio for all speedlines.

$$\text{RMSE} = \sqrt{\frac{1}{N}\sum_{i=1}^{N}\left(\frac{y_i - \hat{y}_i}{\hat{y}_{\max}}\right)^2}, \tag{7}$$

  where $N$ is the total number of points.

- Mean: Mean of the predicted values of mass flow rate and pressure ratio for all speedlines.

## 3 Results and Discussion

| Optimizer | Error Metric | Overall RMSE |
|---|---|---|
| TNC | Ortho | 0.025979 |
| L-BFGS-B | Ortho | 0.025991 |
| Nelder-Mead | Ortho | 0.025991 |
| Nelder-Mead | R2 | 0.025991 |
| Nelder-Mead | MAE | 0.025991 |

Table 2: Top 5 best performers for Pressure Ratio based on Normalized RMSE

As described in the sections above, an overall normalised RMSE was used to compare different configurations with each other. Table 2 and Table 3 show the top 5 performers for each category for the noisest dataset. Out of the 12 configurations, these show the best results for the given task based on overall normalized root mean squared error. The intersection of the two errors show that the optimizer L-BFGS-B with Ortho error metric performs the same as Nelder-Mead with all the error metric.

In terms of accuracy it is evident from the tables that all the configurations can work. In terms of performance, the 12 configurations were evaluated based on the

| Optimizer | Error Metric | Overall RMSE |
|---|---|---|
| L-BFGS-B | Ortho | 0.026964 |
| Nelder-Mead | Ortho | 0.026964 |
| Nelder-Mead | R2 | 0.026964 |
| Nelder-Mead | MAE | 0.026964 |
| Powell | R2 | 0.026967 |

Table 3: Top 5 best performers for Mass flow rate based on Normalized RMSE

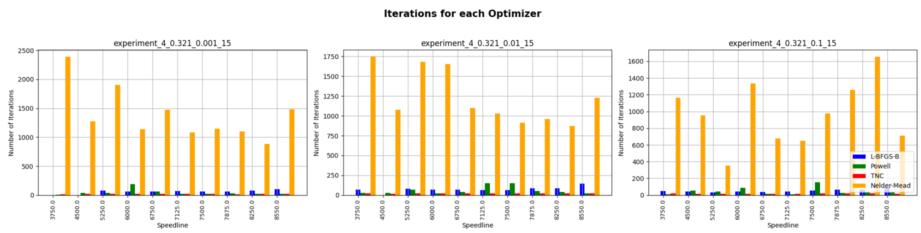


Figure 2: Number of iterations for different optimizers per speedline for the three datasets (Error Metric - Ortho).

number of iterations they take to achieve the minimization. Since the top 2 performers belong to Ortho metric Fig. 2 and Fig. 3 show the comparision. Nelder-Mead being a gradient-free algorithm, takes exceedingly more number of iterations compared to the other chosen gradient-based as well as gradient-free algorithms. More such comparisions can be found in the Appendix.

In Fig. 5, it can be observed that L-BFGS-B optimization algorithm with Ortho as error metric is the optimal configuration for the compressor dataset. The default search space (0.75 to 1.25) was expanded, and the mean of the Mean Square Error (MSE) at different compressor speed for pressure ratio and mass flow rate was analyzed across different boundary conditions. The results indicate that for 0.1 to 2 boundary condition, the mean of the MSE for both pressure ratio and mass flow rate is lower compared to other bounds. Moreover, the reduction in the mean of the MSE for pressure ratio and mass flow rate is *4.34%* and *15.65%*, respectively.

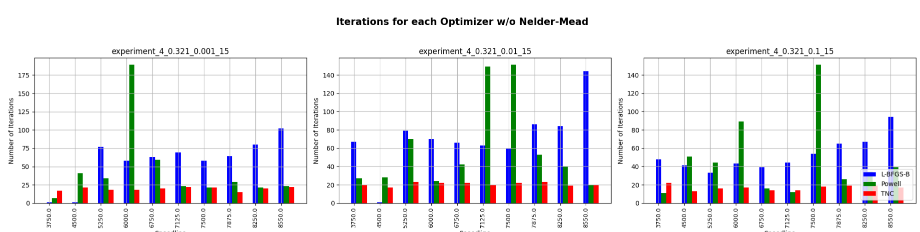


Figure 3: Number of iterations for different optimizers per speedline for the three datasets but without Nelder-Mead (Error Metric - Ortho).

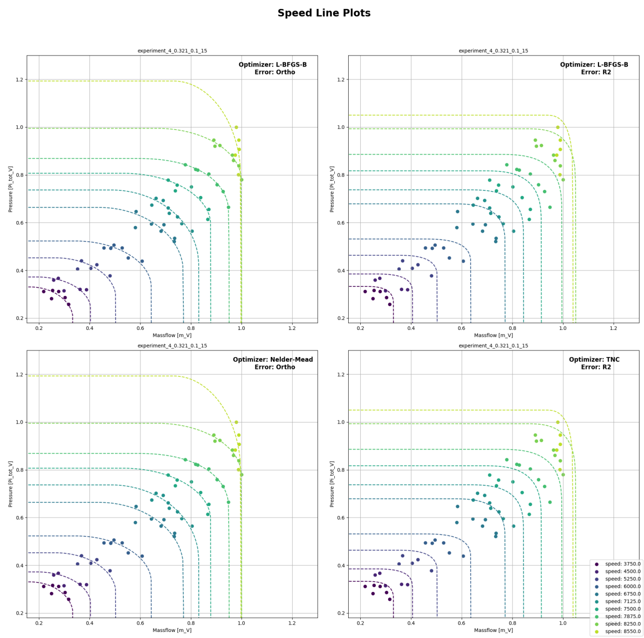


Figure 4: The speedline plots of the best performers (left) and worst performers (right)

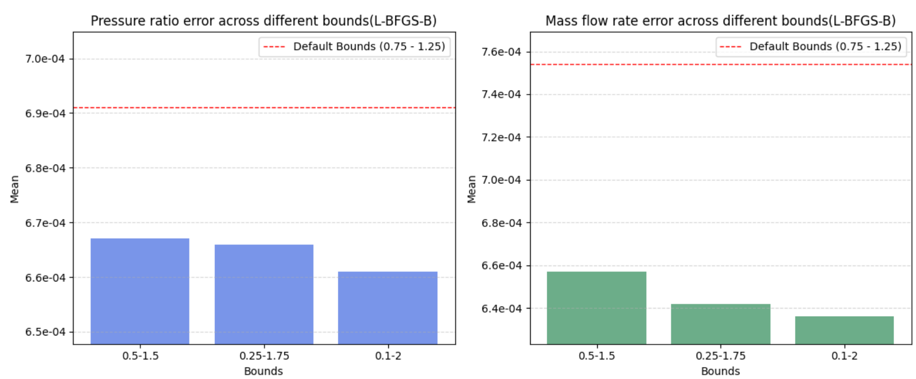


Figure 5: Comparision of different bound settings for L-BFGS-B Ortho.

## References


Xiande Fang, Weiwei Chen, Zhanru Zhou, and Yu Xu. 2014. Empirical models for efficiency and mass flow rate of centrifugal compressors. *International Journal of Refrigeration* 41 (2014), 190–199. doi:10.1016/j.ijrefrig.2014.03.005

Stephen G Nash. 1984. Newton-type minimization via the Lanczos method. *SIAM J. Numer. Anal.* 21, 4 (1984), 770–788.

John A Nelder and Roger Mead. 1965. A simplex method for function minimization. *The computer journal* 7, 4 (1965), 308–313.

Michael JD Powell. 1964. An efficient method for finding the minimum of a function of several variables without calculating derivatives. *The computer journal* 7, 2 (1964), 155–162.

Haosheng Shen, Chuan Zhang, Jundong Zhang, Baicheng Yang, and Baozhu Jia. 2019. Applicable and Comparative Research of Compressor Mass Flow Rate and Isentropic Efficiency Empirical Models to Marine Large-Scale Compressor. *Energies* 13 (12 2019), 47. doi:10.3390/en13010047

Kang Song, Devesh Upadhyay, and Hui Xie. 2019. A physics-based turbocharger model for automotive diesel engine control applications. *Proceedings of the Institution of Mechanical Engineers, Part D* 233, 7 (2019), 1667–1686. doi:10.1177/0954407018770569 arXiv:https://doi.org/10.1177/0954407018770569

Pauli Virtanen, Ralf Gommers, Travis E. Oliphant, Matt Haberland, Tyler Reddy, David Cournapeau, Evgeni Burovski, Pearu Peterson, Warren Weckesser, Jonathan Bright, Stéfan J. van der Walt, Matthew Brett, Joshua Wilson, K. Jarrod Millman, Nikolay Mayorov, Andrew R. J. Nelson, Eric Jones, Robert Kern, Eric Larson, C J Carey, İlhan Polat, Yu Feng, Eric W. Moore, Jake VanderPlas, Denis Laxalde, Josef Perktold, Robert Cimrman, Ian Henriksen, E. A. Quintero, Charles R. Harris, Anne M. Archibald, Antônio H. Ribeiro, Fabian Pedregosa, Paul van Mulbregt, and SciPy 1.0 Contributors. 2020. SciPy 1.0: Fundamental Algorithms for Scientific Computing in Python. *Nature Methods* 17 (2020), 261–272. doi:10.1038/s41592-019-0686-2

Ciyou Zhu, Richard H Byrd, Peihuang Lu, and Jorge Nocedal. 1997. Algorithm 778: L-BFGS-B: Fortran subroutines for large-scale bound-constrained optimization. *ACM Transactions on mathematical software (TOMS)* 23, 4 (1997), 550–560.


## A Online Resources

The software used in this study is available online at:

- `https://github.com/sequential-parameter-optimization/spotoptim`
- `https://github.com/NaitikDalwadi/Numerical-Methods-and-Optimization`.